Journal of Power Sources 195 (2010) 1427–1434

Contents lists available at ScienceDirect

Journal of Power Sources

journal homepage: www.elsevier.com/locate/jpowsour

Fuel sensor-less control of a liquid feed fuel cell under dynamic loading conditions for portable power sources (II)

C.L. Chang[a,*], C.Y. Chen[a], C.C. Sung[b], D.H. Liou[a], C.Y. Chang[a], H.C. Cha[a]

[a] Institute of Nuclear Energy Research (INER), No. 1000, Wunhua Rd., Jiaan Village, Longtan Township, Taoyuan County 32546, Taiwan, ROC
[b] National Taiwan University, Taiwan, ROC

ARTICLE INFO

Article history:
Received 25 August 2009
Accepted 7 September 2009
Available online 15 September 2009

Keywords:
Liquid feed fuel cell
Fuel sensor-less control
Direct methanol fuel cell
Methanol crossover

ABSTRACT

This work presents a new fuel sensor-less control scheme for liquid feed fuel cells that is able to control the supply to a fuel cell system for operation under dynamic loading conditions. The control scheme uses cell-operating characteristics, such as potential, current, and power, to regulate the fuel concentration of a liquid feed fuel cell without the need for a fuel concentration sensor. A current integral technique has been developed to calculate the quantity of fuel required at each monitoring cycle, which can be combined with the concentration regulating process to control the fuel supply for stable operation. As verified by systematic experiments, this scheme can effectively control the fuel supply of a liquid feed fuel cell with reduced response time, even under conditions where the membrane electrolyte assembly (MEA) deteriorates gradually. This advance will aid the commercialization of liquid feed fuel cells and make them more adaptable for use in portable and automotive power units such as laptops, e-bikes, and handicap cars.

1. Introduction

Liquid feed fuel cells, such as the direct methanol fuel cells (DMFCs), have some inherent advantages over conventional power sources, such as power units, for use in mobile, portable, and low power automotive applications. A DMFC uses methanol as fuel rather than hydrogen, eliminating the problem of hydrogen storage, reducing the risk of explosion, and significantly increasing the convenience and safety of fuel cells. Portable products grow with increasing human demand, in that the more functions they have, the more power they consume. A DMFC system is simple (without reformers and humidifiers) and the theoretical energy of methanol is much higher than that of hydrogen and lithium batteries. Therefore, DMFCs have attracted worldwide research attention and are adaptable to portable and automotive applications, such as laptops, PDAs, camcorders, e-bikes, and handicap cars.

The operating characteristics of a DMFC, such as methanol concentration, reactant flow rates, and temperatures of the stack and environment, all considerably influence the behaviors of the DMFC system. Among those operating characteristics, methanol concentration is one key factor that significantly affects the performance and fuel utilization of the DMFC. Methanol crossover from anode to cathode through a Nafion membrane, which causes a mixed potential on the cathode and reduces the overall cell voltage, is a well-known problem that hinders the development of DMFC [1,2]. Due to methanol crossover, practical operation of a DMFC requires accurate control of the methanol concentration within a predetermined range. The conventional approach is to use a methanol concentration sensor in a closed loop of fuel circulation. However, many requirements exist for methanol concentration sensors for DMFC [3]. Existing affordable products that meet all desirable criteria are not yet readily available. Furthermore, methanol sensors that have been developed using electrochemical methods [4] have issues, such as performance degradation of the MEA, which result in poor stability and durability. Methanol sensors based on physical properties, such as sound speed, density, or refractometry, are also sensitive to carbon dioxide bubbles and the pulse wave of the circulation pump in the fuel loop. In addition, methanol concentration sensors, regardless of whether they are designed using physical or electrochemical principles, exhibit a marked dependency on temperature. Measurement efforts and data sets will be large, complicated, and costly for development. Furthermore, when a methanol sensor is used, experimental tasks, such as calibration for each sensor, are necessary. Although the fuel sensor approach can be used to control fuel concentration, it nevertheless has the shortcomings of increased weight, size, complexity, and cost of the liquid feed fuel cell. Accordingly, the development of fuel sensor-less control of liquid feed fuel cells has received much more attention in recent years.

* Corresponding author. Tel.: +886 3 4711400x6855; fax: +886 3 4711409.
E-mail address: clchang@iner.gov.tw (C.L. Chang).

0378-7753/$ – see front matter © 2009 Elsevier B.V. All rights reserved.
doi:10.1016/j.jpowsour.2009.09.012

Nomenclature

F	Faraday's constant (96,480 C mol^{-1})
G	gain factor, determined experimentally
I_n	the nth current load of stack (n = 1, 2, 3, . . ., N) (A)
I_r	reference load
IR-DTFI	impulse response based on discrete time fuel injection
IR-CIDTFI	impulse response based on current integral and discrete time fuel injection
k	compensation factor for fuel consumption during injection delay period
$M(I_n)$	amount of fuel injected at each cycle when subject to load current I_n (mg)
n	number of electrons exchanged
R	correction factor for fuel utilization
T_{ID}	injection duration
T_{IDP}	injection delay period
T_{SMP}	specific monitoring period

Greek symbols

$\eta_{fuel}(I_n)$	fuel utilization at load current I_n
$\eta_{fuel}(I_r)$	fuel utilization at load current I_r

The literature on fuel sensor-less control of liquid feed fuel cells is relatively sparse [5–12]. Our previous investigations [8–9] have discussed most of the developments of fuel sensor-less control for DMFCs. Shen et al. [10] developed a fuel supply control system for DMFCs by calculating a temperature difference between the predetermined working temperature and the fuel area temperature, and then generating a fuel supply speed by adjusting a preset speed according to that temperature difference. This is a special case occurring when the load current is fixed and thus, its applications may be limited whenever the fuel cell system is subjected to dynamic load. Ha et al. [11] presented a sensor-less control logic system that can operate based on estimation of methanol consumption rates for DMFC systems. The calculation of the methanol consumption rate in this paper did not consider the methanol quantity that escapes via vapor from the mixing tank.

Our previous papers [8–9] have presented a fuel sensor-less control algorithm (IR-DTFI) with a fixed injection quantity at each cycle, while the specific monitoring period was modulated to regulate the concentration such that the fuel concentration and power output were controlled within an acceptable range. The specific monitoring periods were equal to or longer than 40 s, namely, the IR-DTFI control algorithm controlled the DMFC system behavior through the system responses of the last cycle of 40 s. The specific monitoring periods depend on the total amount of methanol solution in the mixing tank and the anode compartment of the fuel cell system. We have successfully demonstrated a 40 W DMFC power pack for power sources in notebooks and DVD players that are embedded with the IR-DTFI control scheme for control of fuel supply. In this paper, a modified impulse response based on current integral and discrete time fuel injection control scheme (abbreviated as IR-CIDTFI henceforth) is presented. The fuel injection behavior is treated as an impulse while the response is taken as the control object. The discrete time fuel injection is an important feature for the IR-CIDTFI control scheme. A shortened monitoring period (5 s or less) is explored for faster system response and greater stability. A new current integral technique with a fixed domain for calculating the fuel injection quantity is proposed and validated, which is then successfully combined with the IR-CIDTFI control algorithm to control the fuel supply in DMFCs for low power automotive applications such as e-bikes and handicap cars.

Fig. 1. An experimental 16-cell bipolar plate stack.

2. Experimental

2.1. Stack development

This study adopts two homemade stacks designed and fabricated with conventional bipolar plates and parallel serpentine flow fields [13–15], one of which is a 40 W stack with 20-cells, where each cell contains one commercial product with a five-layer MEA, as shown in Fig. 1; the active area of each MEA is 50 cm^2. The 20-cell stack is used in Sections 3.1 and 3.2. The other is a 25 W stack with 16-cells, which is used in Sections 3.3–3.5. Both stacks show that our DMFC power packs of compact size are suitable for portable power sources.

2.2. The IR-CIDTFI control strategy for the DMFC system under dynamic load conditions

Fig. 2 is a flow chart depicting the steps in the IR-CIDTFI method for supplying fuel to a fuel cell. Fig. 3 shows schematic diagrams of the measurement system, system control, and fuel-feeding unit for verification and evaluation of the IR-CIDTFI control scheme. Our previous work [9–10] has discussed the details regarding the IR-DTFI control scheme, which is similar to the IR-CIDTFI control scheme presented in this paper. The specific monitoring period can be regarded as the response time of the IR-CIDTFI control scheme. The major differences between the control schemes are stated in the following: in step A1, a specific monitoring period (5 s or less) is explored and verified for effective control of the fuel supply. As illustrated in our previous work [9–11], the specific monitoring period is greater than 40 s and the injection quantity is fixed at each monitoring cycle. The IR-CIDTFI control scheme adopts the current integral function for calculating the fuel consumption during each monitoring cycle, shown in step A14. A specific amount of fuel for injection into the fuel cell is calculated according to Eq. (2), which is the current integral function and will be explained in Sections 2.3 and 3.1.

2.3. Relationship between the fuel supply and dynamic load

According to Faraday's Law, electrolysis of the methanol in the DMFC is a function of load current, which is shown in Eq. (1).

$$M_O = \frac{1}{nF}\int Idt \quad (1)$$

where M_O is the amount of methanol electro-oxidized (mol), n is the number of electrons exchanged, F is the Faraday's constant

(96,480 C mol^{-1}), I is the current (A), and t is the time required for the electro-oxidation current to fall from I to zero (s).

Based on Faraday's law, we proposed and developed a current integral equation for calculation of fuel quantity injected at each cycle for the aforementioned IR-CIDTFI control scheme. The general pattern is shown in Eq. (2).

$$M(I_n) = G \times \int_{t0}^{t2} I_n \times R dt + k \times G \times \int_{t2}^{t4} I_n \times R dt, \quad \text{where,}$$
$$R = \frac{\eta_{\text{fuel}}(I_r)}{\eta_{\text{fuel}}(I_n)} \tag{2}$$

where $M(I_n)$ is the amount of fuel injected at each cycle when subjected to load current I_n (g), I_n is the nth current load of DMFC ($n = 1, 2, 3, \ldots, N$) (A), R is the modification factor for fuel utilization, k is the compensation factor for fuel consumption during the injection delay period, t is the time of monitoring period (s), t_0, t_2, t_4 are the time domain boundary conditions for Eq. (2) illustrated in Fig. 4, $\eta_{\text{fuel}}(I_n)$ is the fuel utilization at load current I_n, and I_r is the reference load. G is a function related to the following factors: the unit weight at each injection, the electron transfer number n of the fuel cell electrochemical reaction, the Faraday constant F, and operation parameters as well as system configurations. When the

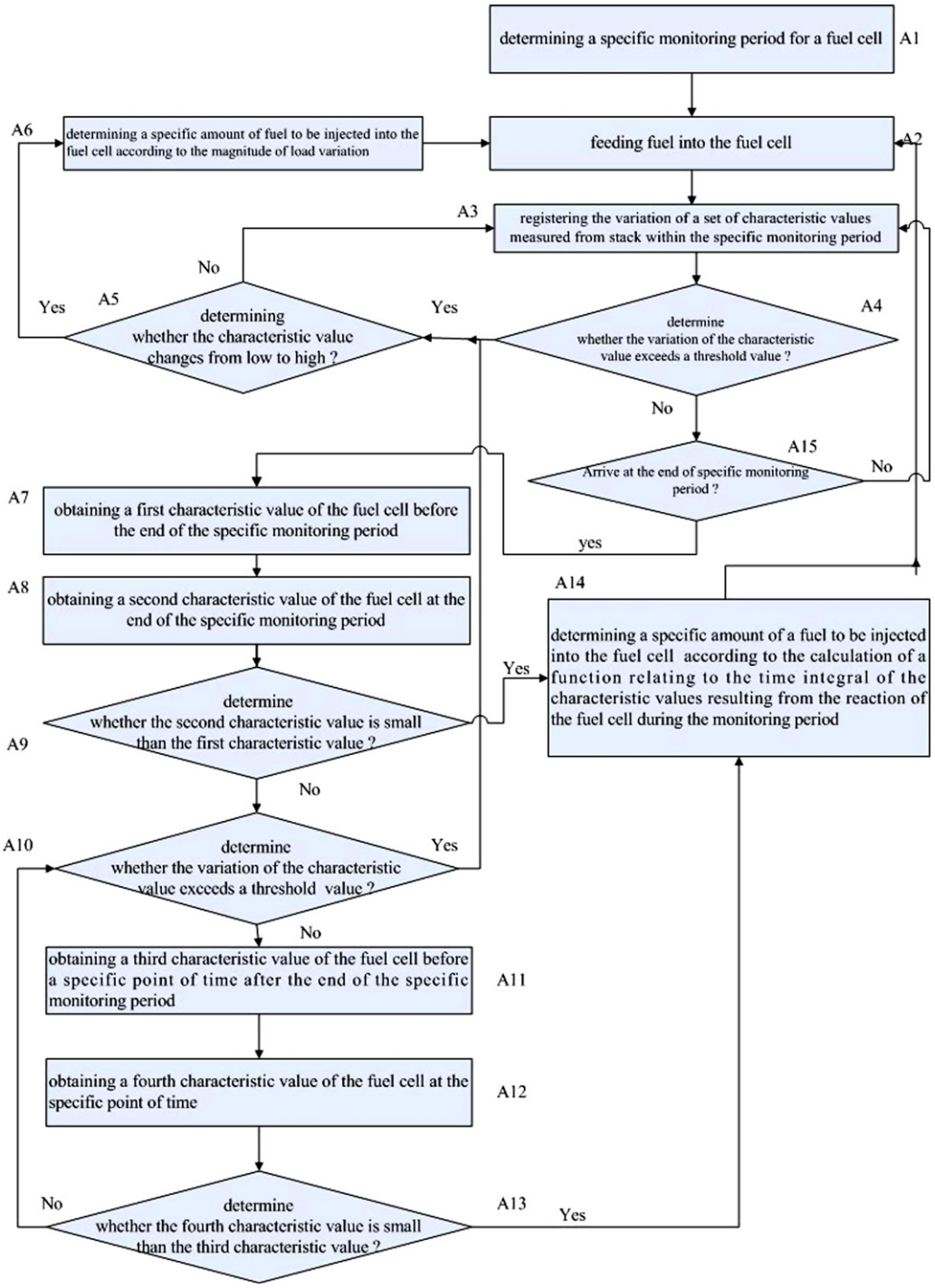

Fig. 2. Flow chart of the IR-CIDTFI control scheme.

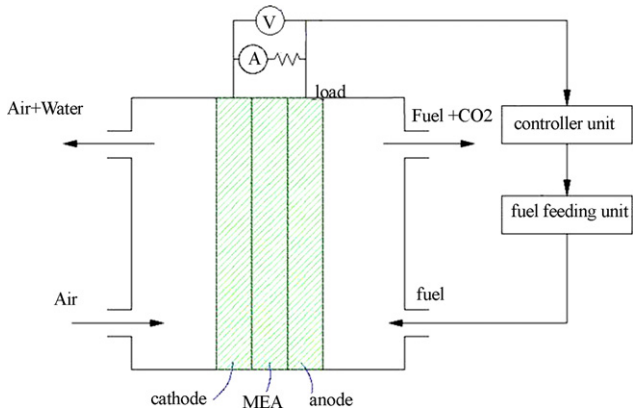

Fig. 3. Schematic diagrams of the measurement system, system control, and fuel-feeding unit for verification and evaluation of the IR-CIDTFI control scheme.

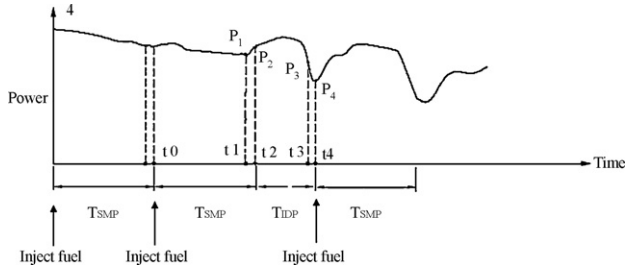

Fig. 4. The typical load profile for current integral at each cycle; t_0 is the time point at which fuel is injected, the duration between t_0 and t_2 is the specific monitoring period (T_{SMP}); the duration between t_2 and t_4 is the injection delay time (T_{IDP}, P1 < P2).

operation parameters and system configurations of the DMFC system are determined, G will be a constant, which can be determined through experiments. The consumption of methanol in the DMFC varies with different loads and can be classified in three parts: oxidation of methanol at the anode, methanol crossover from anode to cathode, and methanol escape as vapor. At any load I_n, the three parts mentioned above can be related to the fuel utilization function $\eta_{fuel}(I_n)$. Our previous work [10–11] has illustrated a method for use of R (modification factor for fuel utilization) to calculate the fuel quantity demanded under dynamic loading conditions, while the fuel utilization function $\eta_{fuel}(I_n)$ at any load I_n can be obtained experimentally in advance. At first, $M(I_r)$ and G values required to sustain the reference load I_r can be found with the R value set to one through experiments. Then, $M(I_n)$ at any low load I_n can be calculated according to Eq. (2).

The first term of Eq. (2) calculates the fuel consumption during the specific monitoring period (T_{SMP}). The second term of Eq. (2), discovered by experiments and explained in Section 3.1, is related to compensation for fuel consumption during the injection delay period (T_{IDP}). Originally, in our previous work [9–10], the second term of Eq. (2) did not exist. The function of the injection delay period was to exhaust excessive fuel that accumulated in the early injection cycles. When the T_{SMP} is reduced from 40 s to 5 s, the unit weight of fuel injected at each cycle can be reduced from 400 mg to 50 mg. The second term of Eq. (2) should function to solve the problem, as seen in Section 3.1. It is worthwhile to note that Eq. (2) is not meant to be used for theoretical prediction of the exact quantity of methanol that the fuel cell consumes at each cycle, but is meant to provide a rational value that can cooperate with the IR-CIDTFI algorithm to control the fuel supply for fuel cell for good load-following characteristics and stable operation.

With regard to application of the current integral equation, there are two kinds of approaches. One is to perform the integral of the load current at a fixed domain (a constant period, such as 5 s). In a fuel cell, the integration of load current during a constant period (5 s) is proportional to the fuel consumption. This work will present this point of view by setting T_{SMP} as a constant while varying the amount of fuel injected at each cycle. Another approach is to perform the load current integral until it reaches a specific value, so that the domain of the current integral can be variable while the amount of fuel injected at each cycle is a constant value, which will be presented in the near future.

2.4. Test apparatus for evaluation of the IR-CIDTFI control algorithm

Fig. 5 shows the test apparatus for evaluation of the IR-CIDTFI control algorithm as applied to the DMFC. The major parts of the instruments are the same as shown in our previous work [10] except that the following items were changed:

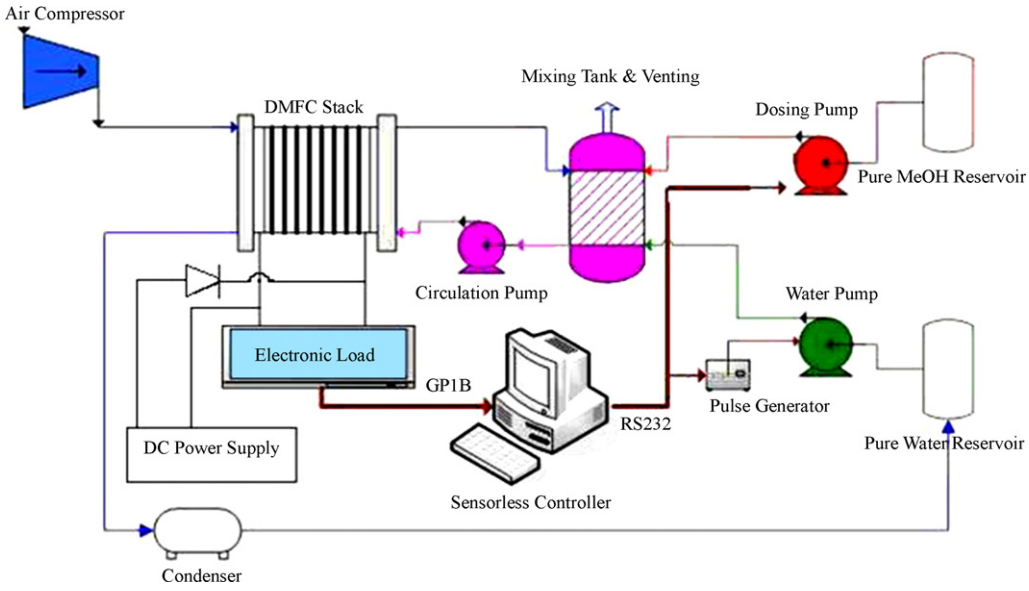

Fig. 5. The test apparatus for evaluating the IR-CIDTFI control algorithm.

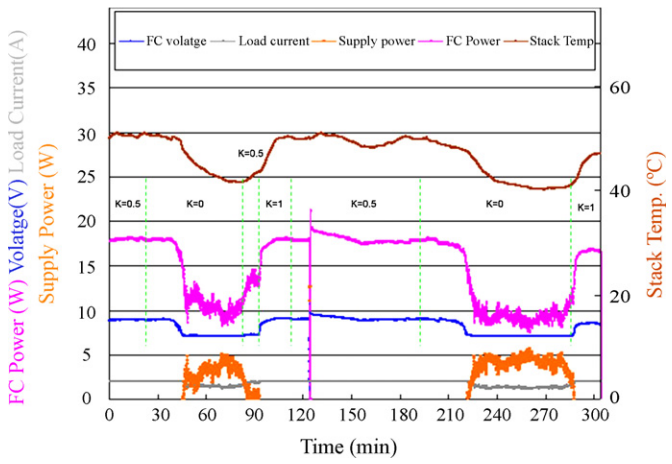

Fig. 6. Operating characteristics of the 20-cell stack under steady load, which is controlled by the IR-CIDTFI algorithm for verifying Eq. (2) (T_{SMP}: 5 s; G: 3.125 (mg (A s)$^{-1}$)).

(1) The second item in previous work [10]: A dosing pump (with fluid transmission, a pure methanol reservoir, and a mixing tank) was serially controlled for injection of methanol into the mixing tank with accuracy of ±2% and changeable flow rate from 30 μL min^{-1} to 30 mL min^{-1}.
(2) The fourth item in previous work [10]: A pulse generator (GW INSTEK PHS-3610) was actuated by a computer and used to generate pulses to drive the water pump.

All experiments were conducted at room temperature (23–28 °C) at a relative humidity of 42–80% with an anode flow rate of 158 mL min^{-1} and a cathode air flow rate of 6 L min^{-1} under the normal ambient conditions of portable electronic devices and automotive applications.

3. Results and discussion

3.1. Steady load test mode

Steady load is currently the most useful load pattern for fuel cell applications. In the steady load test mode, two experiments with different compensation factors have been conducted to realize the effect of compensation factor k on the IR-CIDTFI control algorithm. As shown in Fig. 6, the 20-cell stack is discharged at constant current of 2 A, and the experimental configurations are shown in Table 1. The compensation factor k in Eq. (2) calculates the fuel consumption during the T_{IDP} and affects the load-following characteristics of the IR-CIDTFI control scheme. The power curve of segments 1 and 5 remains flat and acceptable with k set to 0.5. The ratio of the amplitude of the power oscillation to the mean power was about 0.8%, which is spectacularly small as compared with performance figures (4–10%) reported in our previous work [9–11]. This is because the T_{SMP} of our previous works is greater than 40 s with the amount of injection fuel at each cycle measuring about 400 mg. When the T_{SMP} is greatly shortened from 40 s to 5 s, the fuel injection quantity in each monitoring cycle can be reduced from 400 mg to 50 mg, which brings about smaller concentration variation and therefore smaller power fluctuation. In segments 2 and 6, the fuel consumptions during the T_{IDP} are not considered with k set to 0. The power curve dropped dramatically, from 17 W to 10 W, at the 39 min mark in segment 2 and the same phenomena was repeated again at 218 min in segment 6, which signifies insufficient fuel supply. The power curves remain flat during the periods from 20 min to 39 min and 200 min to 218 min because it takes about 18 min to consume enough methanol in the fuel cell system to reach a new lower fuel concentration. In segments 2 and 6, there are no fuel compensations (k = 0) at the end of each T_{IDP}. Based on experimental observations, the injected amount of fuel at each cycle is quite small (50 mg), which often enables the power curve to climb up at the judgment point, 5 s from the start of each cycle. This causes the T_{SMP} to extend from 5 s to 10–20 s quite frequently and results in insufficient fuel supply. This is a problem, as stated in Section 2.3, which caused by the injection quantity and the judgment mechanism in the IR-CIDTFI control scheme, where the fuel consumption during the T_{IDP} is not calculated (k = 0). Therefore, the addition of the second term of Eq. (2), which calculates the fuel consumption during the T_{IDP} as in segments 1 and 5 and injects fuel at the end of each T_{IDP}, helps to compensate for the fuel consumption and solves the problem as seen in segments 2 and 6. In segment 3, the parameter k is changed from 0 to 0.5 for 10 min. The power curve climbs up from 10 W to 14 W and tends to remain at 14 W. It takes more time for recovery from 10 W to 17 W with k set to 0.5. In segment 7, the power climbs rapidly from 10 W to 17 W with k changed from 0 to 1. Therefore, the parameter k clearly affects the load-following characteristics of the DMFC system. This experiment validates the effectiveness of the IR-CIDTFI control algorithm and the current integral function for the DMFC system under steady load. As shown above, the second term of Eq. (2) is necessary, in general, and the following experiment will identify the optimum value of k.

Table 1
Configurations for the validation of the IR-CIDTFI control algorithm and the current integral in Eq. (2) under steady load.

Segment	Time (min)	k
1	0–20	1/2
2	20–80	0
3	80–90	1/2
4	90–110	1
5	110–200	1/2
6	200–280	0
7	280–300	1

Fig. 7 shows the performance test results for finding the optimum parameter k of the fuel compensation factor in Eq. (2) under steady load. The related configurations of the experiment are shown in Table 2. The experiment takes place as follows: the 16-cell stack is discharged at a constant current of 4 A with k set to 1/3, 1/2, 1/6, 1/1, and 1/4 in sequence, and thus, the effect of the fuel compensation factor with regard to the performance of the IR-CIDTFI control algorithm can be measured. There were four 1-min

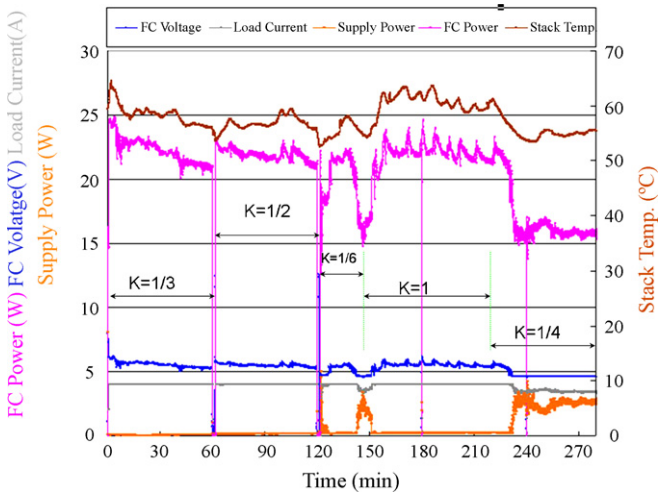

Fig. 7. Performance test for finding the optimum parameter k of the fuel compensation term for Eq. (2) (T_{SMP}: 10 s; G: 3.125 (mg (A s)$^{-1}$)).

Table 2
Configurations for finding the optimum parameter k for the fuel compensation term in Eq. (2) under steady load.

Segment	Time (min)	k
1	0–60	1/3
2	61–120	1/2
3	121–150	1/6
4	151–220	1/1
5	221–280	1/4

breaks in this experiment for recovery from temporary degradation of the MEAs. The power profiles of segments 3 and 5 show declining trends in the curves, which translate to insufficient fuel supply. The power and temperature profiles of segment 4 with $k = 1$ show some fluctuations, which signals excessive fuel supply that still can be regulated by the IR-CIDTFI control algorithm. Only the power profiles of segments 1 and 2 are stable, with little fluctuations as compared to the other segments. Therefore, for a steady load, the optimum value for fuel compensation factor k would exist between 0.5 and 0.34. When subjected to an increasing load, the DMFC system may demand more fuel for good load-following characteristics such that $k = 1$ would be a more suitable choice.

3.2. Dynamic load test mode

In order to investigate feasibility of the IR-CIDTFI control scheme and the current integral function under dynamic loads, the test loads were scheduled to switch between 1 A and 4 A in sequences with a period of 60 min. The test configuration shown in Table 3 includes various combinations of fuel supplies to evaluate the effect of correction factor R for fuel utilization in Eq. (2). The 1 A load was used to simulate the BOP load, and 4 A was used to simulate full load. The fuel utilization at 4 A and 1 A were measured to be 0.68 and 0.52, respectively. Fig. 8 shows the experimental results. In segments 2 and 6, the fuel supplies were tuned to be just adequate to sustain the high load of 4 A with R set to 1, which is taken as a reference standard for the fuel supply calculation in the other segments. When the fuel supply quantity for the high load of 4 A is obtained through experiments, Eq. (2) can be applied to calculate the quantity of fuel supply for the low load of 1 A with R set to 1.31 (=0.68/0.52), which is set in segments 1 and 3. The power profiles of segments 1, 2, 3, and 6 show good performances with little fluctuations, as compared with other segments, because their fuel supply calculations were just enough to sustain the loads. The fuel supply for 4 A in segments 4 and 8 were excessive with R set to 1.31, and the power profiles fluctuated to a large extent, where the high concentration of fuel still could be regulated by the IR-CIDTFI control scheme. The fuel supplies for 1 A in segments 5 and 7 were insufficient with R set to 1 (i.e., without fuel utilization correction) and thus the power curves decayed with negative slope

Table 3
Experimental parameters for the evaluation of R (modification factor of fuel utilization) in the IR-CIDTFI control scheme, when the 16-cell stack was subjected to dynamic load.

Segment	Time (min)	Fuel efficiency correction factor (R)	Load current (A)
1	0–60	1.31	1
2	61–120	1	4
3	121–180	1.31	1
4	181–240	1.31	4
5	241–300	1	1
6	301–360	1	4
7	361–420	1	1
8	421–480	1.31	4

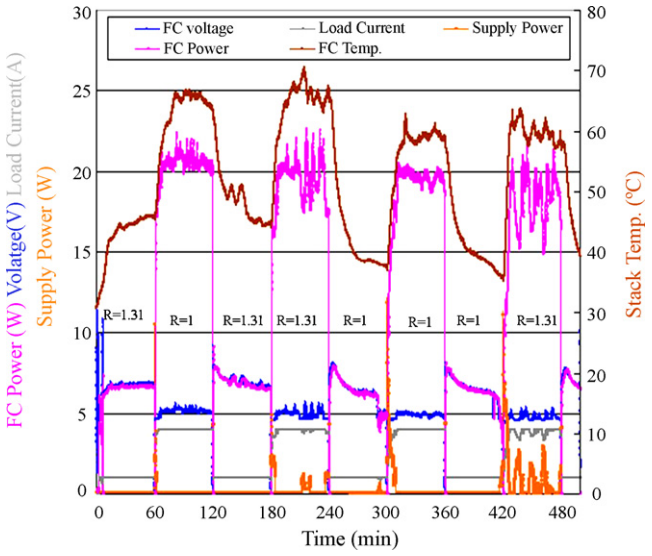

Fig. 8. Effect of R (the correction factor for fuel utilization) on the IR-CIDTFI control scheme, when the 16-cell stack was subjected to dynamic load (T_{SMP}: 10 s; G: 3.125 (mg (A s)$^{-1}$), $k = 0.5$).

and both dropped suddenly at the time intervals of 287–300 min and 410–420 min, respectively.

3.3. Ladder step load test mode

In Sections 3.3 and 3.4, the 20-cell stack is used as the test unit. Three experiments are designed to investigate the load-following characteristics of the IR-CIDTFI algorithm under the ladder step loads and pulse loads. An empirical formula (3) for the fuel utilization function (η_{fuel}) of the 20-cell stack was obtained by curve fitting of discrete load data.

$$\eta_{fuel}(I) = 0.0492 + 0.873 \times I - 0.6 \times I^2 + 0.21 \times I^3 - 0.035 \times I^4 + 0.0022 \times I^5 \quad (0.2 < I < 5.1) \tag{3}$$

Fig. 9 shows the performance test results of the 20-cell stack under the ladder steps load which starts from 0.5 A to 5 A with a step of 0.5 A. The value of R at different loads can be calculated by way of the empirical formula (3). The cumulative injection times are plotted in blue triangles in Figs. 9 and 10. Thus, the horizontal

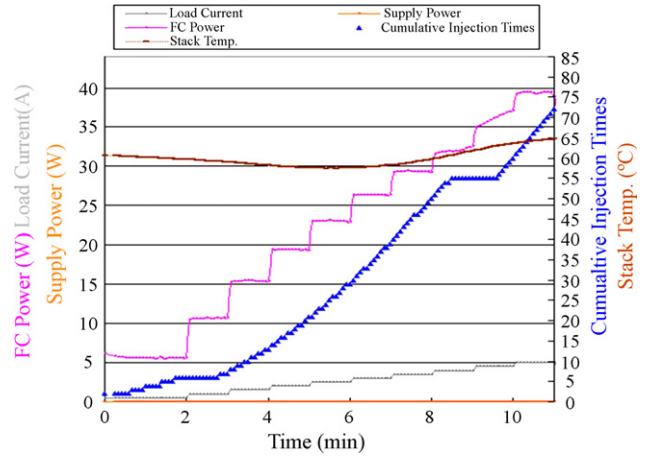

Fig. 9. Dynamic response of the 20-cell stack subjected to ladder step increasing load with the fuel supply under the IR-CIDTFI algorithm control (T_{SMP}: 5 s; G: 3.125 (mg (A s)$^{-1}$), $k = 0.5$).

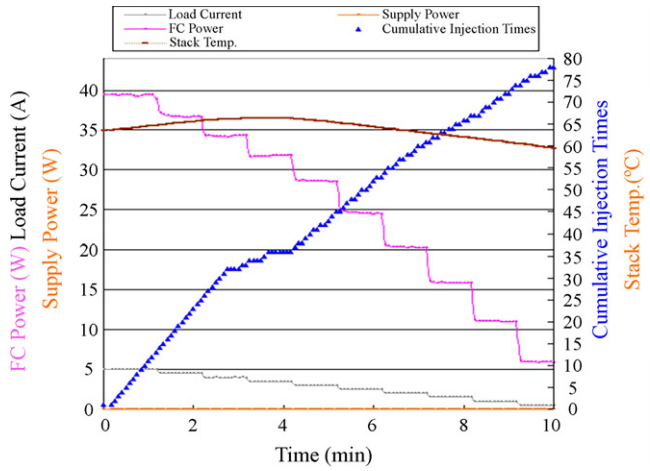

Fig. 10. Dynamic response of the 20-cell stack subjected to ladder step decreasing load with the fuel supply under the IR-CIDTFI algorithm control (T_{SMP}: 5 s; G: 3.125 (mg (A s)$^{-1}$), k = 0.5).

length of each of the blue bars represents the period between two consecutive injections at each monitoring cycle. As shown in Fig. 9, two significant injection delay periods are found to regulate concentration in 1 A and 4.5 A in situations that last for about 1 min. During those injection delay periods, no further fuel is fed into the mixing tank and the excessive fuels are regulated gradually in those periods.

Fig. 10 shows the performance test results of the 20-cell stack under ladder step loads, which start from 5 A and proceed down to 0.5 A with a step of 0.5 A. As portrayed in Fig. 10, three significant injection delays occurred in the 4 A and 3.5 A regions that regulated the fuel concentration. The power and temperature curves of Figs. 9 and 10 show that the stack operates normally with little fluctuations while injection delays, triggered by the IR-CIDTFI control scheme, occur occasionally to regulate the fuel concentration.

3.4. Pulse load test mode

Fig. 11 shows the transient responses of a 20-cell stack subjected to five sets of pulse load. The load pattern is designed to simulate the switching behaviors that occur between different levels of a multilevel charger and with frequent on-off switching. When the charger is switched off, the load is sufficient only to sustain the BOP. When a pulse load change occurs from a low current to a relative

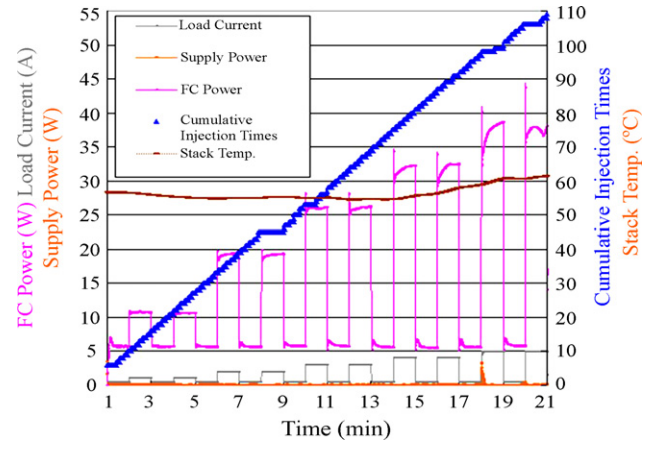

Fig. 11. Dynamic response of the 20-cell stack subjected to pulse load with the fuel supply under the IR-CIDTFI algorithm control (T_{SMP}: 5 s; G: 3.125 (mg (A s)$^{-1}$), k = 0.5).

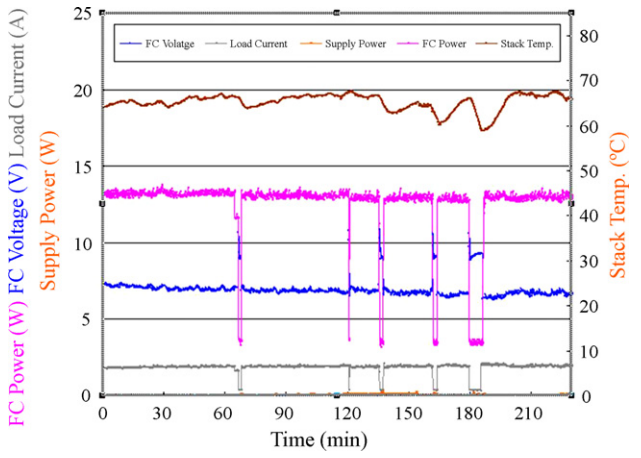

Fig. 12. Performance of the 16-cell stack as a power source for a DVD player under IR-CIDTFI algorithm control (T_{SMP}: 10 s; G: 3.125 (mg (A s)$^{-1}$), k = 0.5. R = 1.09 for DVD player load, R = 1.35 for BOP).

high current, the voltage and power response gradually approaches the steady-state value at relatively high current load, but tends to show a sharp rise at low current load that results in an overshoot and slow relaxation back to the steady-state value. The R value at different loads can be calculated according to empirical formula (3). There are three significant injection delays, triggered by the IR-CIDTFI control algorithm, in the periods of 8–9 min, 18–19 min, and 20–21 min, which regulate the methanol concentration occasionally. From the above experiments, the fuel supplies are efficient for the dynamic loads, and the response time and power fluctuations are greatly reduced as compared with those data presented in our previous works [9–11].

3.5. DVD player load test mode

Fig. 12 plots the performance characteristics of the 16-cell stack with a real load using a DVD player and BOP for 220-min operation. The DVD player was switched on and off randomly. The BOP consumed approximately 3.5 W and the DVD player consumed 8–10 W. When the DVD player was switched on, the stack output was maintained stably at approximately 13–14 W output under the control of the IR-CIDTFI algorithm. When the DVD player was switched off, the stack outputted approximately 3.5 W for BOP operation, which caused the temperature of the stack to drop drastically. The power output was stable and its fluctuation was small, mainly caused by the variations of load current and fuel concentration. The experimental result of the DVD player load test demonstrated that the IR-CIDTFI algorithm effectively controlled the supply of methanol under real loading conditions.

Judging from the temperature and power responses of all experiments, we can conclude that the methanol concentrations are controlled within acceptable range. There is no need for concern regarding the fuel concentration with the application of the IR-CIDTFI control algorithm during the operation of a liquid feed fuel cell. The control algorithm results in power fluctuations that are key features of the IR-CIDTFI control scheme. These fluctuations are measured at the stack terminal and could be regulated through the conditioning circuit for the load. Further study in the near future will show that the current integral function can be implemented in a fixed quantity in such as way that the fuel injection quantity is fixed at each monitoring cycle while the duration between two injections varies.

Experimental results systematically confirm that the IR-CIDTFI control algorithm can control the DMFC such that it functions well under both steady and dynamic loading. Fig. 13 shows a DVD player

Fig. 13. Demonstration of a DVD player powered by a 40 W DMFC system.

Table 4
System characteristics of the DMFC power source for DVD player demonstrated by INER.

Power	80 W
Output voltage	25 V
Weight	3 kg
Size	101 × 147 × 295 mm^3 (4.4 L)
Fuel	100 wt.% MeOH, 500 c.c.
Operating temperature	60–70 °C
Continuous operation	8–10 h

powered by a 40 W DMFC power system that embedded with our fuel sensor-less control algorithm. The detailed system characteristics used to power the DVD player are listed in Table 4, and we were able to demonstrate it successfully in July 2008.

4. Concluding remarks

The IR-CIDTFI algorithm, an innovative fuel sensor-less control scheme for a liquid feed fuel cell system under dynamic loading conditions, has been presented and verified experimentally. Detailed control processes, implementation considerations, and experimental results are presented with the IR-CIDTFI control scheme. A new load current integral function with a fixed domain has been validated, which calculates the amount of fuel consumed during the last monitoring cycle and makes the DMFC system more adaptable to dynamic loading conditions. A more shortened response time of 5 s has been implemented successfully in our DMFC power pack. Notably, the IR-CIDTFI control algorithm can survive even when the stack degrades continuously. It is simple, easy to comprehend, and if implemented in liquid feed fuel cells, would benefit the development of DMFCs. Consequently, the advantages of the IR-CIDTFI control algorithm, such as reduced weight, volume, and cost of DMFC, extended lifetime, increased reliability, and simplified control algorithm, makes the liquid feed fuel cell system highly promising for portable and low power automotive applications.

Acknowledgements

The authors are grateful for the financial support from the Institute of Nuclear Energy Research (INER), Taiwan, ROC

References

[1] L. Jorrissen, V. Gogel, J. Kerres, J. Garche, J. Power Sources 105 (2002) 267.
[2] A. Heinzel, V.M. Barragan, J. Power Sources 84 (1999) 70.
[3] H. Zhao, J. Shen, J. Zhang, H. Wang, D.P. Wilkinson, C.E. Gu, J. Power Sources 159 (2006) 626–636.
[4] S.R. Narayanan, W. Chun, T.I. Valdez, US Patent 6,306,285 (2001).
[5] W.P. Acker, M.S. Adler, S. Gottesfeld, US Patent 6,991,865 (2006).
[6] J. Zhang, K.M. Colbow, A. Wong, B. Lin, US Patent 6,698,278.(2004).
[7] Y.J. Chiu, H.C. Lien, J. Power Sources 159 (2006) 1162–1168.
[8] C.L. Chang, C.Y. Chen, C.C. Sung, D.H. Liou, J. Power Sources 164 (2007) 606–613.
[9] C.L. Chang, C.Y. Chen, C.C. Sung, D.H. Liou, J. Power Sources 182 (2008) 133–140.
[10] S.Y. Shen, L.F. Chang, K.Y. Kang, C.C. Lai, TW Patent I282639 (2005).
[11] Tae Jung Ha, Jong-Ho Kim, Han-Ik Joh, Soo-Kil Kim, Go-Young Moon, Tae-Hoon Lim, Chong-hun Han, Heung Yong Ha, Int. J. Hydrogen Energy 33 (2008) 7163–7171.
[12] C.Y. Chen, D.H. Liu, C.L. Huang, C.L. Chang, J. Power Sources 167 (2007) 442–449.
[13] C.Y. Chen, C.S. Tsao, Int. J. Hydrogen Energy 31 (2006) 391–398.
[14] C.Y. Chen, P. Yang, Y.S. Lee, K.F. Lin, J. Power Sources 141 (2005) 24–29.
[15] C.Y. Chen, P. Yang, J. Power Sources 123 (2003) 37–42.